



ALMA MATER STUDIORUM  
UNIVERSITÀ DI BOLOGNA

ARCHIVIO ISTITUZIONALE  
DELLA RICERCA

Alma Mater Studiorum Università di Bologna  
Archivio istituzionale della ricerca

Morphology of setae in regenerating caudal adhesive pads of the gecko *Lygodactylus capensis* (Smith, 1849)

This is the final peer-reviewed author's accepted manuscript (postprint) of the following publication:

*Published Version:*

Morphology of setae in regenerating caudal adhesive pads of the gecko *Lygodactylus capensis* (Smith, 1849) / Alibardi L.; Bonfitto A.. - In: ZOOLOGY. - ISSN 0944-2006. - ELETTRONICO. - 133:(2019), pp. 1-9. [10.1016/j.zool.2019.01.003]

*Availability:*

This version is available at: <https://hdl.handle.net/11585/709328> since: 2021-12-01

*Published:*

DOI: <http://doi.org/10.1016/j.zool.2019.01.003>

*Terms of use:*

Some rights reserved. The terms and conditions for the reuse of this version of the manuscript are specified in the publishing policy. For all terms of use and more information see the publisher's website.

This item was downloaded from IRIS Università di Bologna (<https://cris.unibo.it/>).  
When citing, please refer to the published version.

(Article begins on next page)

This is the final peer-reviewed accepted manuscript of

Alibardi L.; Bonfitto A.: Morphology of setae in regenerating caudal adhesive pads of the gecko  
*Lygodactylus capensis* (Smith, 1849). ZOOLOGY 133. ISSN 0944-2006

DOI: 10.1016/j.zool.2019.01.003

The final published version is available online at: <http://dx.doi.org/10.1016/j.zool.2019.01.003>

**Rights / License:**The terms and conditions for the reuse of this version of the manuscript are specified in the publishing policy. For all terms of use and more information see the publisher's website.

*This item was downloaded from IRIS Università di Bologna (<https://cris.unibo.it/>)*

***When citing, please refer to the published version.***

# Morphology of setae in regenerating caudal adhesive pads of the gecko *Lygodactylus capensis* (Smith, 1849)

Lorenzo Alibardi<sup>a,\*</sup>, Antonio Bonfitto<sup>b</sup>

<sup>a</sup> *Comparative Histolab Padova, Italy*

<sup>b</sup> *Department of Biological, Geological and Environmental Sciences (BiGeA), Bologna, Italy*

## ARTICLE INFO

gecko  
tail pads  
regeneration  
immunolabeling  
ultrastructure

## ABSTRACT

After tail loss in the African gecko *Lygodactylus capensis* (Smith, 1949) a new tail is regenerated, including caudal adhesive pads. The axial skeleton of the regenerating tail consists in an elastic cartilaginous tube replacing the original vertebrae that allows interacting with the substrate like in the original tail. The formation of adhesive setae has been analyzed using transmission and scanning electron microscopy coupled to immunolabeling for Corneous Beta Proteins. During progressive stages of epidermal differentiation new setae are developed at stage 4 of the shedding cycle and contain Corneous Beta Proteins. These structural proteins are faintly localized in the Oberhäutchen but are abundant in the beta-layer, indicating that the two epidermal layers have a different protein composition. The setae originate from the growth of Oberhäutchen spinulae into the cytoplasm of clear cells and the latter produce a thick fibrous meshwork of keratin and other unknown proteins localized around the growing setae. This cytoskeleton likely allows molding tail setae like for digital setae. A graded development of setae is observed from the base to the tip of regenerated pads and from the periphery to more central areas. The terminal end of the setae is subdivided into numerous filamentous spatulae that increase the adhesion contact. Sensory boutons are frequently detected at the margin of tail scales and adhesive pads, likely improving compliance with the substrate. The present study indicates that tail regeneration is a convenient experimental model to analyze adhesive setae formation, microstructures that allow to these lizards climbing vertical and arboreal substrates.

## 1. Introduction

Among the modified scales of lizards, the formation of soft and sticky outer (dorsal) surfaces, occurs in adhesive pads, as summarized in Maderson, 1964, 1970) and Russel (2002). These pads are usually found in digits that are utilized for clinging and climbing onto almost any type of substrate, allowing to these geckos to move on vertical and inverted surfaces and defeating gravity (Autumn and Peattie, 2002; Russel, 2002; Gao et al., 2005; Niewiaroski et al., 2016). The external layer of these adhesive digital scales, the outer scale surface, presents micro-ornamentation derived from the most external layer of the epi dermis, called Oberhäutchen. These microstructures grow in length for 5 to above 100  $\mu\text{m}$ , depending from the species (Maderson, 1970), and form long bristles termed setae that terminate with an enlarged adhesive nanostructure, the spatula (Rizzo et al., 2006; Alibardi, 2009,200; Alibardi, 2018; Alibardi and Meyer Rochow, 2017). The cellular process at the origin of setae remains unknown but previous comparative ultrastructural studies on different species of

lizards have indicated the formation of a cytoskeletal meshwork around the growing setae while they accumulate large amounts of Corneous Beta Proteins, a family of small proteins previously indicated as beta keratins (Alibardi, 1999; Alibardi and Meyer Rochow, 2017). The study on the origin of these microstructures has become important also for various technological applications, and numerous studies have been carried out aiming to produce artificial materials of multiple utilizations with adhesive properties similar to those of geckos (Ge et al., 2007; Autumn and Gravish, 2008; Carbone et al., 2011).

In addition to digital pads some geckos also possess adhesive pads by the tip of the tail, as summarized by Maderson (1971), and Bauer, (1998). Caudal adhesive pads were initially described since the end of the 19<sup>th</sup> Century by Tornier (1899) and from other subsequent authors (Muller, 1910; Schmidt, 1919; FitzSimons, 1943; Mertens, 1964) in numerous species of geckos. This anatomical specialization further helps these lizards to move across the arboreal environment where they live. Since the tail can also regenerate in case of loss, also normal scales and even those modified as pads can regenerate (Mertens, 1964;

\* Corresponding author at: Department of Biological, Geological and Environmental Sciences (BiGeA), via Selmi 3, 40126 Bologna, Italy.  
E-mail address: lorenzo.alibardi@unibo.it (L. Alibardi).

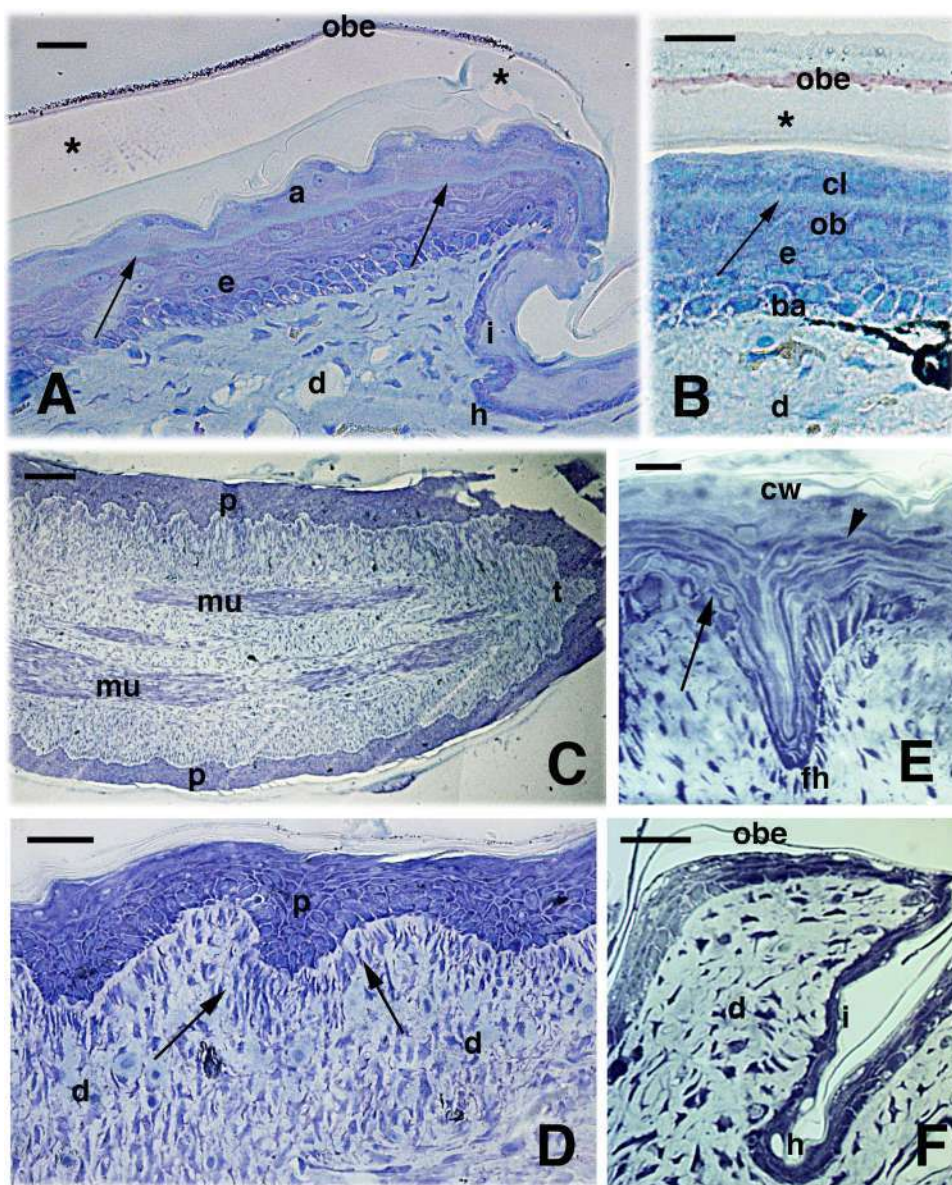


**Fig. 1.** Histology of normal tail scales (A-B) and on progressive stages of scale regeneration (C-F). **A**, beginning of formation of the shedding line (arrows) within the epidermis. Bar, 10  $\mu$ m. **B**, detail on the shedding line (arrow) separating the clear from the Oberhäutchen. Bar, 10  $\mu$ m. **C**, regenerating tail at 25 days of regeneration showing the wound epidermis forming pegs. Bar, 50  $\mu$ m. **D**, detail on peg elongation at 25 days, from right to left, with the oriented fibroblasts (arrows) in the forming dermis. Bar, 20  $\mu$ m. **E**, detail on layer stratification within a peg at 25 days of regeneration. The arrow points to presumptive spindle-shaped Oberhäutchen-beta-cells. The arrowhead indicates presumptive clear cells. Bar, 10  $\mu$ m. **F**, regenerated (neogenic) scale with a thin Oberhäutchen-beta-layer located above an incomplete alpha-layer at 35 days of regeneration. Bar, 20  $\mu$ m. **Legends:** ba, basal layer; cl, clear layer; cw, corneous layer of the wound epidermis; d, dermis; e, epidermis; h, hinge region (interscale); i, inner scale surface; mu, regenerating muscles; ob, Oberhäutchen; obe, Oberhäutchen-beta layer; p, epidermal peg; t, tip of the tail; asterisks indicate an artifact detachment of the outer layer due to sectioning.

Maderson, 1971; Alibardi and Meyer Rochow, 2017). Tail regeneration in lizards allows the new formation of numerous tissues and in particular of neogenic scales in the skin (Maderson et al., 1978; Bellairs and Bryant, 1985; Alibardi, 2010). Regenerating scales derive from an invagination of the epidermis into the dermis, and this process give rise to epithelial pegs that progressively generate the new epidermal layers of the new scales, although these are smaller and often irregularly distributed with respect to the original ones (Bryant and Bellairs, 1967; Liu and Maneely, 1969; Alibardi and Toni, 2006; Wu et al., 2014). During regeneration an epidermal generation made of six main layers are produced, indicated from outside inward as Oberhäutchen, beta layer, mesos layer, and finally the alpha layer that is subdivided into a lacunar, alpha mature and clear layer (Maderson et al., 1978, 1998; Alibardi and Toni, 2006). The latter layer forms a temporary connection with the Oberhäutchen layer of the following epidermal generation, a connection that is destined to be eventually degraded at molting. The cells of the clear layer of the outer epidermal generation, destined to molt, initially forms inter digitations with the Oberhäutchen of the successive generation, the inner generation, destined to replace the outer generation at shedding; the two layers form the so called “shedding complex”, a unique specialization of squamates (Maderson et al.,

1998). The shedding complex of adhesive pads is complicated by the elongation of the micro ornamentation of the Oberhäutchen into long setae.

The study of regenerating scales and adhesive pads in geckos can provide further details on the cytological process of formation and shedding in these specialized scales, and in the present study we focus on this experimental system to analyze in particular the origin of setae using immunohistochemistry and electron microscopy, a stage that was missing in a previous study on another species of gecko (Alibardi and Meyer Rochow, 2017). The study confirms that working on regenerating scales and adhesive pads is a useful experimental system for future studies on the role of the cytoskeleton for the origin of the setae.

## 2. Materials and Methods

### 2.1. Animals and fixation

Two juvenile specimens of the African gecko *Lygodactylus capensis* (Smith, 1849) were utilized for this study. The animals were purchased in an authorized pet shop, and they were kept in cages at Summer temperatures (25-30 °C), and fed with small earthworms alternated to

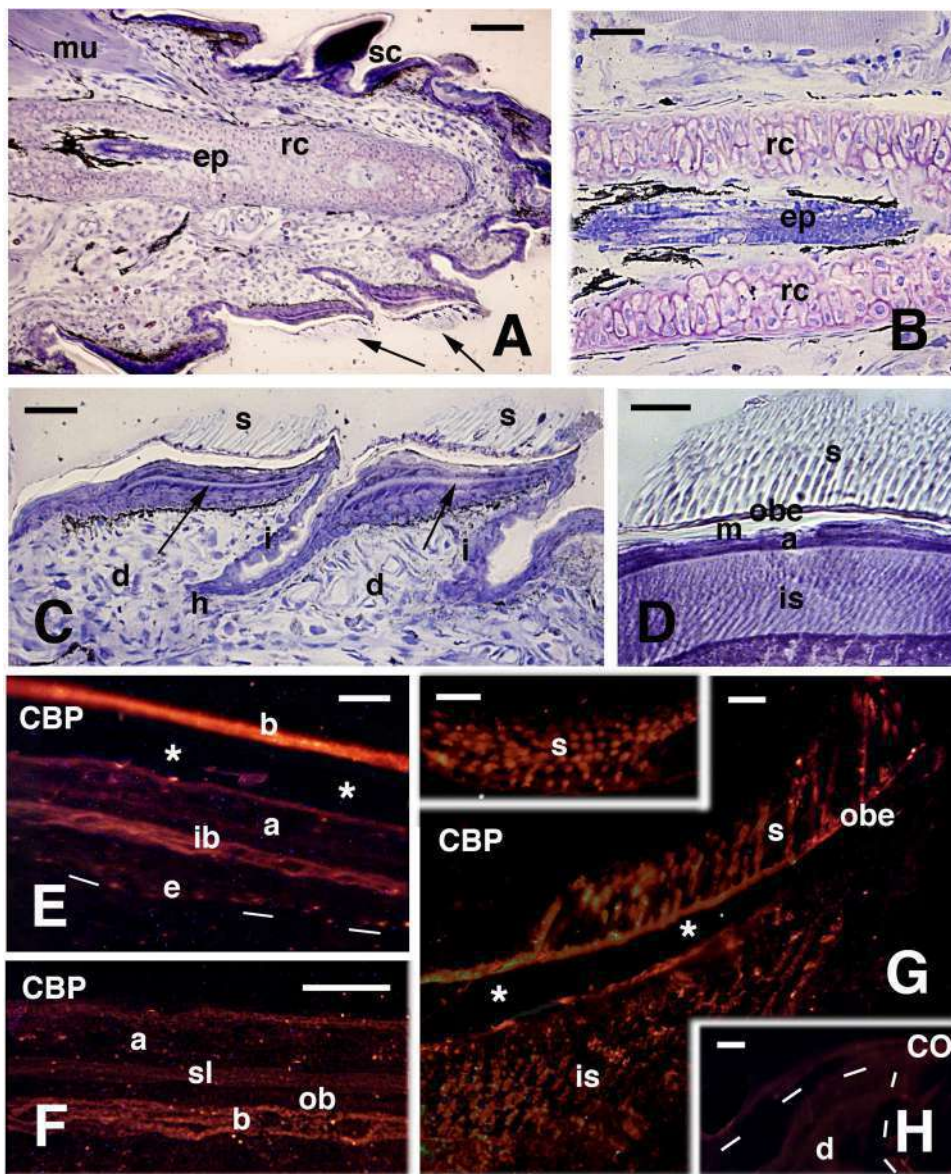


**Fig. 2.** Histology of regenerating tail and adhesive pads (A-D) and immunofluorescence (TRITC) for Corneous Beta Proteins (CBP, E-H) at 35 days of regeneration. **A**, general aspect of the tip of a regenerating tail with the axial cartilage and a well scaled new epidermis. The arrows point to two pads. Bar, 50 μm. **B**, detail on the axial cartilage (metachromatic) with the enclosed ependymal canal. Bar, 20 μm. **C**, close image of two pads featuring the mature and unstained, outer setae, and the shedding line (arrows). Bar, 20 μm. **D**, close-up image of the inner setae present in a caudal pad. Bar, 10 μm. **E**, normal tail scale showing the highest immunofluorescence over the outer beta-layer and the inner beta-layer. Dashes underline the epidermis. Bar, 10 μm. **F**, closer view of the inner beta-layer and of the weakly stained shedding line in a normal scale. Bar, 10 μm. **G**, section of a pad showing intensely labeled outer setae, and their sustaining Oberhäutchen-beta layer. Also the forming inner setae appeared intensely labeled. Bar, 10 μm. In the inset (Bar, 10 μm) most outer setae have been cut in cross section. **H**, immunonegative control section (CO) of normal scale. Dashes underline the epidermis. Bar, 10 μm. **Legends:** a, alpha-layer (mature); b, beta-layer; d, dermis; e, epidermis; ep, ependymal; h, hinge region; i, inner scale surface; ib, inner (forming) beta-layer; is, inner (forming) setae; m, mesos-layer; mu, muscles; ob, Oberhäutchen; obe, Oberhäutchen-beta layer; rc, regenerated cartilage; s, setae (fully cornified); sc, scale; sl, shedding line; asterisks indicate an artifact detachment of the outer layer due to sectioning.

vinegar flies (*Drosophila*) and small crickets. The amputation of the tail was done inducing autotomy near the tail tip and the collected normal tail of about 3 mm was immediately fixed for histology. The regenerating tails were collected from one individual at 25 days (2 mm long), when the skin appeared smooth and un scaled. From the other individual a regenerating tail of 3 mm was collected at 35 days, when it was showing some scaling in the proximal part attached to the original tail. A second round of collection from the same individuals was done on regenerating tails of about 2 mm in length after 35 days from the second amputation in one gecko, and another regenerated tail of 45 days and about 2 mm in length from the second gecko: therefore in total four samples at different regenerative periods (25, 35 and 45 days) were studied in order to capture progressive stages of scale regeneration, and in particular of setae formation in caudal scales.

The collected tails were delicately halved with a sharp scalpel for improving fixation and embedded in Bioacryl resin (Scala et al., 1992) for Histology and TEM (transmission electron microscopy), aside few sampled of the normal and regenerated tail that were kept for the study under SEM (scanning electron microscopy). Fixation was done for 10-12 hours at 4 °C in 5% formaldehyde in 0.2 M Phosphate buffer at pH 7.4, then tissues were dehydrated in ethanol, immersed in Bioacryl for 3-4 hours, and then were inserted into gelatin capsules and exposed at

4 °C to UV light for 2 days for hardening the resin. Other samples of the skin of normal tails (n = 2) and regenerated tail (at 45 days of regeneration, n = 1) were instead dehydrated 2-3 times in pure ethanol, dried at room temperature and prepared for Scanning Electron Microscopy.

## 2.2. Histology and Immunohistochemistry

The tissues in resin were sectioned at 2-4 μm using a Leika Nova ultramicrotome for histology and immunohistochemistry. In the first case the collected sections were stained with 1% Toluidine blue while for immunohistochemistry they were collected over a film of distilled water, dried for about 2 hours on a hot plate at about 40 °C, and reacted with the antibody. The pre core box antibody raised in rabbit (see details in Alibardi and Meyer Rochow, 2017) was utilized for detecting corneous beta proteins (formerly indicated as beta keratins), at a dilution of 1:50-100 in 0.05 M Tris Buffer at pH 7.4, containing 5% of BSA (Bovine Serum Albumin) and 2% NGS (normal goat serum). In order to inhibit non specific antigenic sites, a pre incubation of 30 minutes was done in the incubating solution without the primary antibody. In controls sections, the incubating solution did not contain the primary antibody. After the incubation with the primary antibody and three rinses

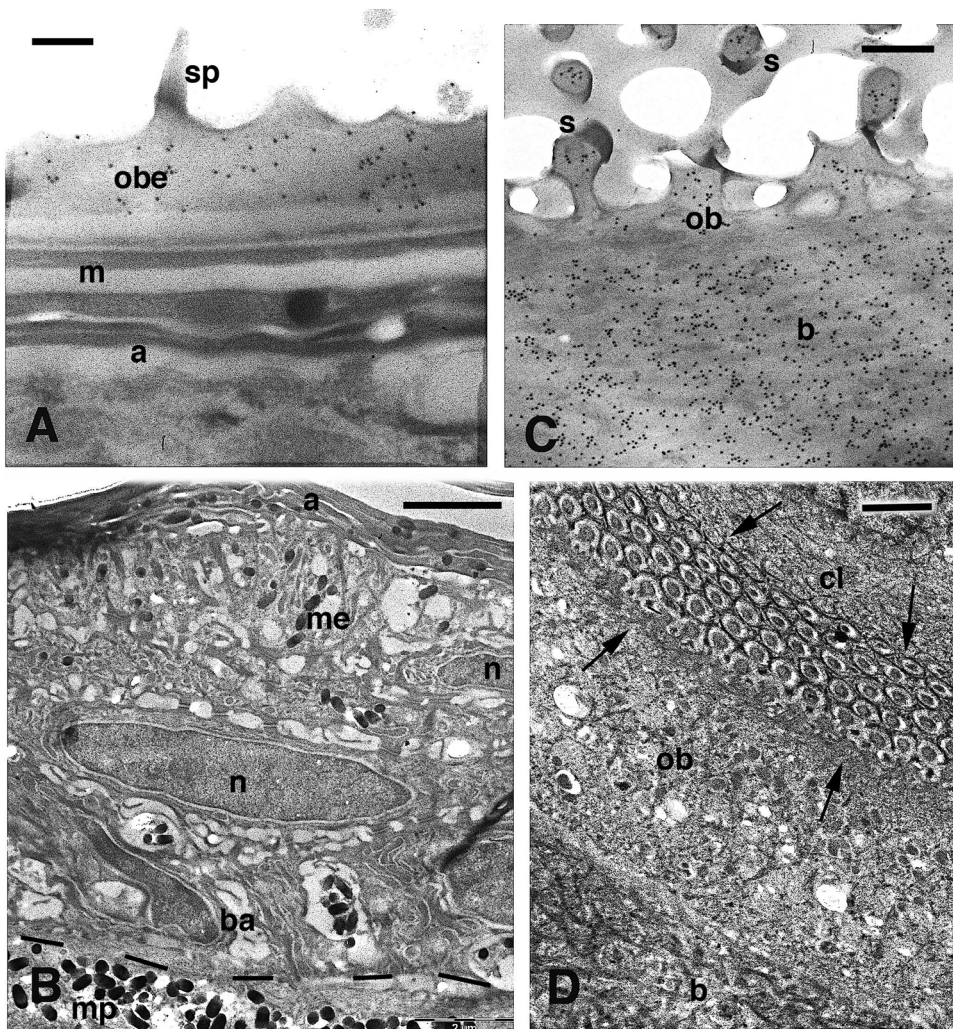


**Fig. 3.** Transmission electron microscopy images on the surface of normal scale epidermis (A-B) and of a regenerating pad (C-D), studied using immunogold labeling for Corneous Beta Proteins. A, labeled Oberhäutchen-beta layer, but not in the spinulae and the underlying (alpha-) layers. Bar, 0,25  $\mu\text{m}$ . B, lower part of the epidermis showing some layers of the alpha-stratum and of pre-corneous and basal cells located underneath. Dashes underline the epidermis. Bar, 2  $\mu\text{m}$ . C, intensely labeled Oberhäutchen-beta layer, including the setae of an adhesive pad. Bar, 0,5  $\mu\text{m}$ . D, general view of the shedding line (between arrows) formed between the clear layer above and the Oberhäutchen below. Bar, 2  $\mu\text{m}$ . **Legends:** a, mature alpha-layer; b, beta-layer; ba, basal layer of the epidermis; cl, clear layer; m, mesos-layer; me, melanosomes; mp, melanophore in the dermis; n, nucleus; ob, Oberhäutchen; obe, Oberhäutchen-beta layer; sp, spinula.

with the buffer, a secondary antibody conjugated to TRITC (Tetra-methyl Rhodamine, Sigma, USA) was applied to the sections at 1:200 dilution for about 1 h at room temperature. Observations were carried out using a fluorescence microscope with a Rhodamine filter, and images were recorded on a digital camera.

### 2.3. Transmission and scanning electron microscopy

For transmission electron microscopy immunogold labeling, thin sections of the tissues were collected on Nickel grids (200 300 mesh) at 40 90 nm thickness. The sections on grids were initially pre incubated for 10 minutes in an incubating solution containing 5% cold Water Fish Gelatin in 0.1 M phosphate buffer at pH 7.2-7.4. The following incubation with the pre core box antibody lasted for 6 hours at room temperature, using a dilution of 1:100 in the incubating solution. In controls the primary antibody was omitted. After rinsing, a goat anti-rabbit secondary antibody conjugated to 20 nm large gold particles was applied to the sections at 1:100 dilution in buffer for 1 h at room temperature. After rinsing in buffer and in distilled water, the dried grids were observed using a Zeiss 10C/CR transmission electron microscope operating at 40 60 kV. Images were collected with a digital camera, and selected images served to compose the figure plates using the Adobe Photoshop program 8.0. For SEM, the dehydrated samples were dried in air, and later coated with Gold using a BIO RAD Sem Coating System SC502 working at 12 mA for 60 sec. and observed under a SEM Hitachi S 2400 operating at 20 kV.

## 3. Results

### 3.1. Light microscopy and immunocytochemistry

The present description briefly summarized the principal and new observations, and more detailed descriptions of normal and regenerating scales have been amply published (Maderon et al., 1978, 1998; Alibardi et al., 2004; Alibardi and Toni, 2006). The histology of normal scales in the sampled tail tips showed the coexistence of two epidermal generations, an incomplete outer generation and a forming inner generation, separated by a pale line that represents the shedding layer between the two generations (Fig. 1 A, B). The outer generation comprised a thin Oberhäutchen beta layer, followed underneath by an immature alpha layer (not yet completely cornified), and terminating with a clear layer that appeared separated from the large polygonal cells of the inner Oberhäutchen layer of the incomplete inner generation by the pale shedding line (Fig. 1 B). The nature of the shedding line was later confirmed under the electron microscope observation (see later description).

The regeneration of the new tail tip was followed until from 25 to 45 days post amputation in *Lygodactylus capensis* at the employed temperatures, and the tail tip was initially (25 days of regeneration) covered by a linear multilayered epidermis which became wavy and formed pegs in more proximal direction (Fig. 1 C). These pegs became asymmetric moving proximally, at about 1 mm from the tail tip, and fibroblasts underneath appeared stretched perpendicularly to the epithelium. In more differentiated pegs at 35 days, the epidermis showed a

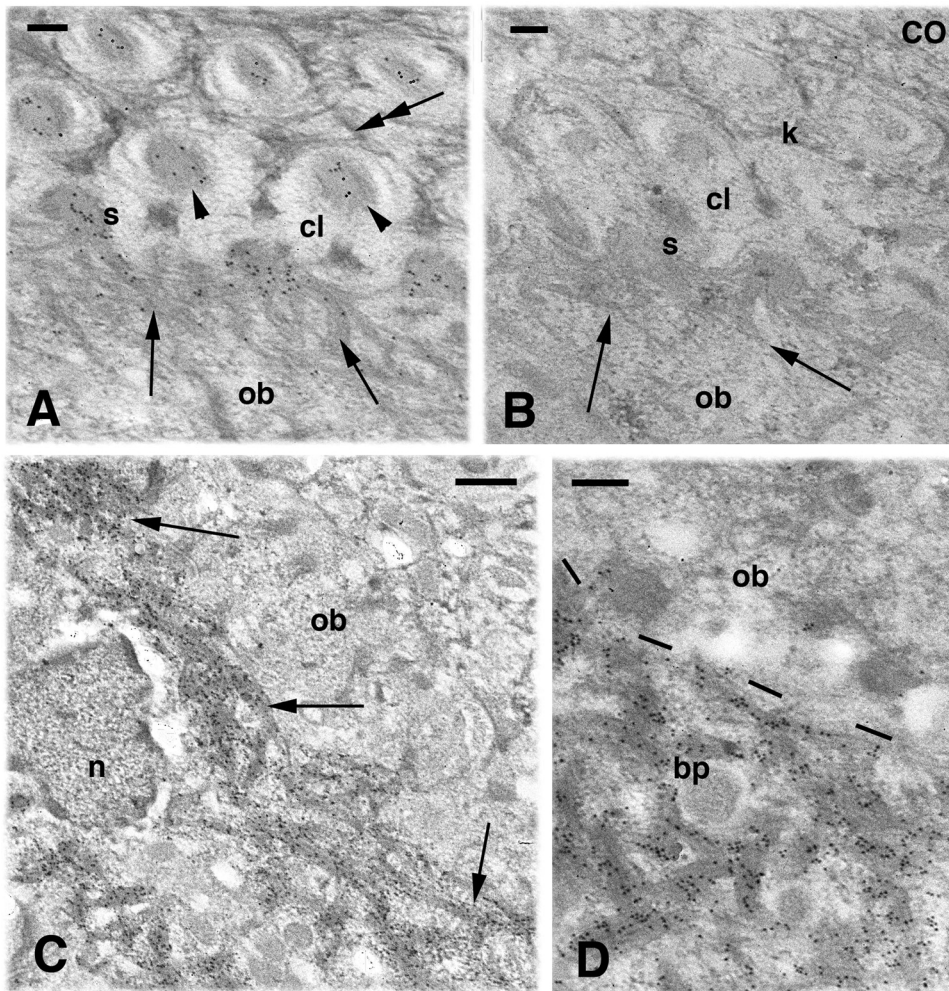


**Fig. 4.** Immunogold labeling for Corneous Beta Proteins in the forming setae. **A**, detail of the shedding line featuring the immunolabeled corneous material incorporating into the developing setae (arrows). Arrowhead indicate cross-sectioned setae while the double arrow point to the denser fibrous meshwork surrounding the setae. Bar, 200 nm. **B**, Immunonegative control (CO) section of centered on the shedding line. Bar, 200 nm. **C**, low magnification image showing beta-cells rich in gold-labeled bundles of corneous material (beta-packets), in continuity (arrows) with the immunonegative Oberhäutchen layer. Bar, 0.5  $\mu$ m. **D**, detail on the intensely labeled beta-packets of a differentiating beta-cells (dashes outline the boundary with an immune-negative Oberhäutchen cell). Bar, 200 nm. **Legends:** cl, clear layer/cytoplasm; k, keratin bundles; n, nucleus; ob, Oberhäutchen layer; s, forming setae.

stratification of new layers, starting with the spindle shaped cells of the new beta generation (Fig. 1 E). The latter eventually packed into a compact but very thin beta layer (Fig. 1 F), that covered the largely formed but still immature neogenic (regenerating) scales at 35 and 45 days (Fig. 1 F).

The histological examination revealed that the axial skeleton of the tail at 25 45 days of regeneration was formed by an elastic type of cartilage, very cellular and with scarce intercellular and metachromatic matrix, that enchased an ependymal epithelium (Fig. 2 A, B). The latter included roundish paler cells, identified as Cerebro Spinal Contacting Neurons (data not shown). Among most normal scales, also those showing longer extensions of pale and unstained bristles, the adhesive pads, were seen in the ventral region of the regenerated tail tip (Fig. 2 A, C). The length of the setae increased abruptly toward the tip of the pad. The pale shedding line consisted in weakly stained setae of 2 4  $\mu$ m in length, generally shorter than the outer setae (Fig. 2 C). In some pads at 35 days however, the inner setae were almost as long as those of the outer generation and the alpha layer appeared mature and largely cornified (Fig. 2 D). This histological condition suggests that these regenerated pads were close to shedding. At 45 days only one generation of setae was seen, as the pads were completely regenerated.

After immunostaining, normal scales showed intensely fluorescent the outer beta layer and also intense was the fluorescence observed on the differentiating and fusiform beta cells of the inner generation (Fig. 2 E, F). Also, the shedding line showed a weak fluorescence while no other part of the epidermis or dermis was labeled. The regenerated scales showed an intense fluorescence in both outer and inner setae, and in the Oberhäutchen beta layer sustaining the setae (Fig. 2 G).

Control sections of normal scales or pads were not immunofluorescent (Fig. 2 H).

### 3.2. Transmission electron microscopy and immunogold

In normal tail scales, the mature and compact Oberhäutchen beta layer was variably labeled while no gold particles were seen in the remaining layers present underneath, including the mature alpha layer (Fig. 3 A, B). The mature Oberhäutchen beta layer of regenerated scales and pads at 35 days was intensely immunolabeled, especially the lower beta component while the merged superficial Oberhäutchen and its setae were less labeled (Fig. 3 C). In regenerating pads at 35 days, the plane of sectioning often intercepted the forming shedding line of pads tangentially, revealing numerous cross sectioned setae of the innergeneration that formed 4 5 rows of circular structures (Fig. 3 D).

The observation at higher magnification revealed that these inner-setae were immunolabeled with gold particles, and also the base of the forming setae accumulated labeled corneous material (Fig. 4 A). This labeling revealed that Corneous Beta Proteins are accumulated in the forming setae. Each seta was surrounded by the pale cytoplasm of clear cells that contained a dense meshwork of fibrous material similar to keratins bundles, with a circular disposition around the setae (Fig. 4 A). No labeling was instead seen in either clear cells surrounding the setae or in control sections (Fig. 4 B).

The remaining cytoplasm of the Oberhäutchen cells was poorly and diffusely labeled for Corneous Beta Proteins while the highest immune labeling was present in the forming beta layer located underneath the shedding line (Fig. 4 C, D). Differentiating beta cells were packed with

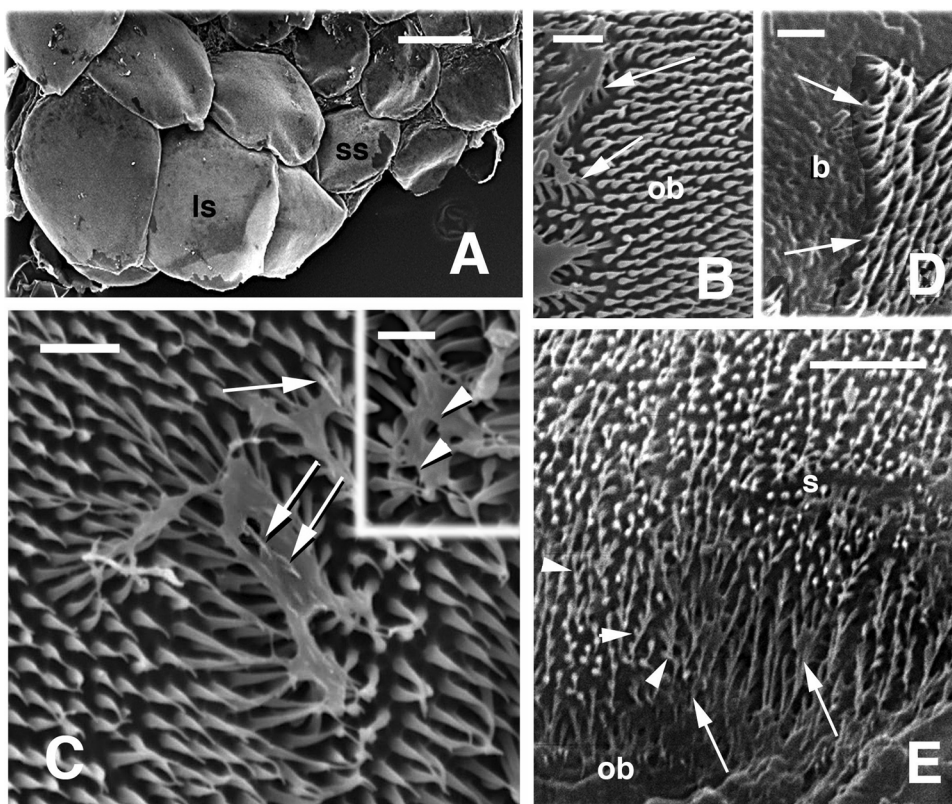


**Fig. 5.** Scanning electron microscopy of caudal scale in regenerated tails. **A**, general view showing variations in the scale size. Bar, 250  $\mu\text{m}$ . **B**, detail on the Oberhäutchen spinulae of a normal scale. Arrows indicate the point of merging of the spinulae with fragments likely left from the clear layer after shedding. Bar, 2  $\mu\text{m}$ . **C**, close up image to show the tip of spinulae (arrows) inserted in cell fragments, likely clear cell remnants. Bar, 2  $\mu\text{m}$ . The inset (Bar, 1  $\mu\text{m}$ ) shows numerous holes (arrowheads) in a cell fragment, likely left from Oberhäutchen spinulae during penetration into the clear layer. **D**, other detail of a fractured area revealing the beta-layer underneath the spinulae (arrows). Bar, 2.5  $\mu\text{m}$ . **E**, longer Oberhäutchen elongation observed in tail scale that shows a branching pattern (arrows) and the formation of rows of terminal club-like, spatula endings (arrowheads). Bar, 10  $\mu\text{m}$ . **Legends:** b, beta-layer; ls, larger scale; ss, smaller scale; ob, Oberhäutchen spinulae; s, setae.

slightly more electron dense and large bundles of corneous material than in Oberhäutchen cells (Fig. 4 D). These bundles merged into a compact and highly immunolabeled beta layer in more differentiated scales at 45 days of regeneration, like for regenerated scales at 35 days (Fig. 3 C).

### 3.3. SEM observations on normal and regenerated scales

The observations at low magnification of normal scales of different size (Fig. 5 A) showed over most of scales a spinulated surface, generated from the Oberhäutchen (Fig. 5 B, C). These spinulae were about 1.5–2.0  $\mu\text{m}$  high and tended to curve backward, sometimes intercepting and perforating occasional fragments the shed clear layer (Fig. 5 B, C). In fact, the observation of these fragments often showed that the sharp tips of the Oberhäutchen spinulae had formed holes in these fragments (Fig. 5 C and the inset). In some scales an unusual pattern of micro-ornamentation was observed, representing microstructures generated from the Oberhäutchen layer in the range of 5–15  $\mu\text{m}$  in length. The latter consisted in some elongation from the Oberhäutchen with a peculiar branching pattern of thin filaments of 0.3–0.5  $\mu\text{m}$  in diameter, and along these branches a series of terminal clubs were formed, perhaps representing a type of spatula ends (Fig. 5 E). Therefore the surface of these scales appeared covered with tiny club-like endings of 0.2–0.4  $\mu\text{m}$  in diameter, a frequent size for spatula endings in gecko setae.

Fully formed pads were observed at the tip of the regenerated tail at 45 days (Figs. 6 and 7). Various pads were seen concentrated by the tail tip, mainly on the ventral surface (Fig. 6 A), and each pad showed numerous cylindrical shaped setae of 30–40  $\mu\text{m}$  in length for a diameter of 1–2  $\mu\text{m}$ . The setae were localized toward the tip of the outer (dorsal) surface, from about the half of the distal region of these modified scales, and terminated at their tip forming a linear row of setae (Fig. 6 B). Along the right and left borders of these modified scales, setae decreased in length and diameter to the size of spinulae (Fig. 6 B, C). The decrement in size was also present toward the proximal surface of the

scales, otherwise covered by small Oberhäutchen spinulae. The setae appeared either isolated or clumped into bundles of 2–6 setae, and also single setae were present (Fig. 6 B, C, D). The irregularity of these clumping indicated that this is an artifact derived from preparation for SEM. Like the more elaborated digital setae, also the caudal setae terminated into a tufts of smaller filaments of 50–150 nm, each terminating in a spatula surface (Figs. 6 D, E, 7 A). High magnification observations showed that by the apical part of each seta, from about 3–6  $\mu\text{m}$  from the tip, branched into 3–6 smaller branches that eventually terminated in 3–6 spatular surfaces in each branch.

At the tip of pads, only long setae were seen, a broad contrast with the much smaller spinulae present in the inner scale surface at the tip of these pads (Figs. 6 B, 7 B, E). Also, along the tip of some tail scales and pads, 1 up to 5 ampullary sensory organs were detected (Fig. 6 B, 7 C, D, E). The ampullae were enclosed in seemingly concavities, and consisted in a circular array of Oberhäutchen spinulae bearing a central tuft of 3–5 long filaments with the size of small setae, 15–20  $\mu\text{m}$  in length by 0.5  $\mu\text{m}$  in diameter each (Fig. 7 D, E).

## 4. Discussion

### 4.1. Caudal setae formation

Compared to previous reports (Maderson, 1971; Alibardi and Meyer-Rochow, 2017), the present study has detected the key stage in which spinulae are forming in normal scales and also pads where setae are forming at 35 days of tail regeneration, corresponding to stage 4 of the epidermal shedding cycle (Maderson, 1964, 1970; Maderson et al., 1998). The present electron microscopic observations, coupled to immunolabeling for Corneous Beta Proteins, confirm that setae contain these small proteins with a central beta sheet region, and that a dense fibrous cytoskeletal meshwork present in the cytoplasm of clear cells surrounds the growing setae, like during the differentiation of the digital setae (Hiller, 1972; Alibardi, 1999, 2003, 2009; Alibardi, 2018; Alibardi and Meyer-Rochow, 2017; Rizzo et al., 2006). The present



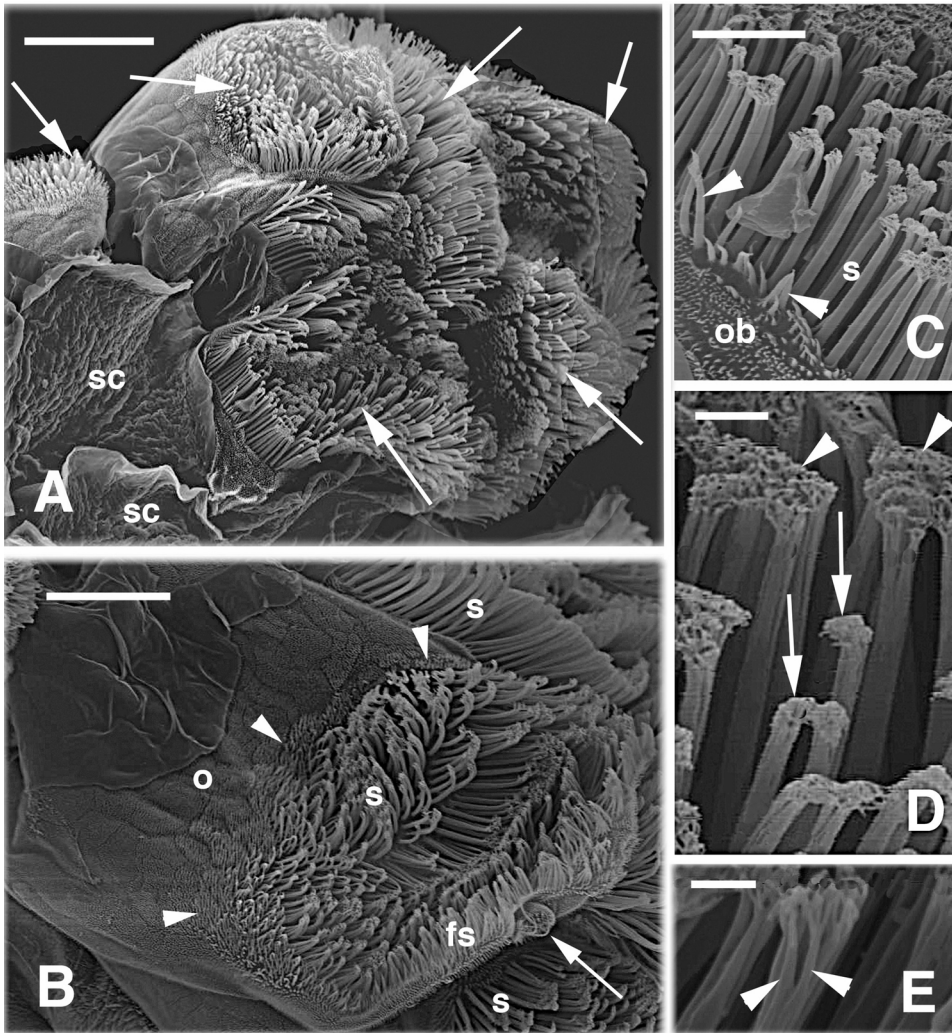


**Fig. 6.** Scanning electron microscopy images on regenerated pads and setae at 45 days. **A**, a group of pads covered by a bed of setae (arrows), and located by the tip of the regenerated tail. Bar, 100  $\mu\text{m}$ . **B**, a single pad shows a group of setae on the tip of the scale, surrounded by smaller spinulae. The arrow indicates an apical sensory organ. Bar, 50  $\mu\text{m}$ . **C**, detail on a row of setae that confine with smaller setae (arrowheads) and more peripherally with small Oberhäutchen spinulae. Bar, 25  $\mu\text{m}$ . **D**, detail on the fluffy tip of isolated (arrows) or clumped (arrowheads) setae. Bar, 5  $\mu\text{m}$ . **E**, other detail on the terminal branching (arrowheads) of setae. Bar, 2  $\mu\text{m}$ . **Legends:** fs, front setae; o, outer (dorsal) scale surface; ob, Oberhäutchen; s, setae; sc, scales.

study shows that the cytoskeleton present inside clear cells contains keratin fibrils but also other, unknown components. It is believed that this cytoskeletal reinforcement of the cytoplasm surrounding the growing setae contributes to their molding into definitive setae and for shaping the terminal end termed spatula, the site of adhesion on the substrate (Alibardi, 1999; Rizzo et al., 2006). The nature of the non-keratinous cytoskeletal material remains unknown but this caudal model of pad morphogenesis appears appropriate for analyzing protein composition in future studies.

The study using the pre core box antibody has shown a weak labeling in the corneous material accumulated in Oberhäutchen cytoplasm, in the spinulae of normal scales, but increases in the setae of adhesive pads. However, the immune localization of Corneous Beta Proteins in setae is lower in comparison to that detected in beta cells during differentiation and after their complete maturation into a compact beta layer. This observation further indicates a different composition of the Corneous Beta Proteins synthesized in the two different layers, although eventually they merge in a syncytium at maturity, here indicated as Oberhäutchen beta layer (obe, see Fig. 1). This difference was previously detected in both lizard and snake Oberhäutchen, which contains granules of dense corneous material rich in sulfur, absent in beta cells (see summary in Alibardi and Toni, 2006). The Oberhäutchen incorporates more histidine than the beta layer, another indication that some histidin rich proteins are accumulated among keratin bundles. Conversely beta cells take up proline in much higher degree than the Oberhäutchen (Alibardi et al., 2004; Alibardi et al. 2004). In snakes, the Oberhäutchen contains some unique Corneous Beta Proteins rich in

cysteine that are absent in the beta layer (Alibardi, 2014). The Oberhäutchen constitutes the layer of transition between the alpha and the beta epidermal generation, and therefore unique proteins are synthesized in this monolayer of transitional cells. Most of proteins in the Oberhäutchen remain to be characterized, but they are likely responsible for the huge variation in micro ornamentation patterns formed in different species of squamates (Price, 1982; Irish et al., 1988; Arnold, 2002). The smaller setae degrading to spinulae size (Fig. 6 B, C), suggest a progressive lateral growth of the setae, especially those present in the proximal area of these modified scales. The static images cannot tell us whether the short setae represent a series of growing (regenerating) setae or merely the termination of the area where setae are located. The former hypothesis is suggested by the localization of mRNAs for Corneous Beta Proteins in the inner and also outer setae, and from the uptake of tritiated histidine in setae (Alibardi et al., 2007).

#### 4.2. Caudal setae morphology in relation to adhesion and sensorial reception

The present SEM observations have revealed a micro ornamentation pattern never seen before in other squamates to the best of the present authors' knowledge, with branching micro ornamentation that appear to give off to rows of endings along the branching system of these thin setae like structures. It is uncertain whether the scales containing this elaborated micro ornamentation (Fig. 5 E) represent a transition from the Oberhäutchen of normal scales and pads or a stage of development of pads from normal scales. Whether this system may enhance further

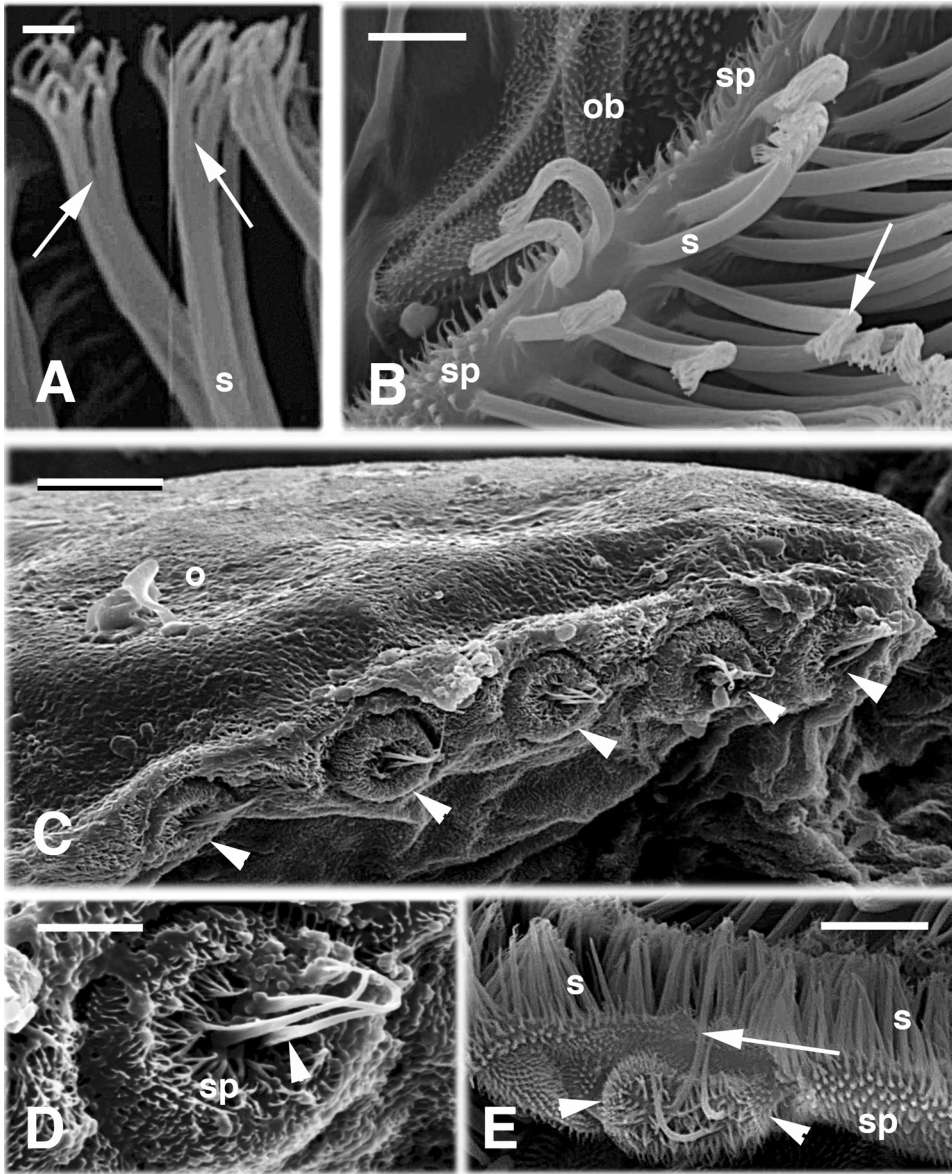


**Fig. 7.** Other scanning electron microscopy images on regenerated pads and setae at 45 days. **A**, high magnification detail on the terminal branching (arrows) of setae. Bar, 1  $\mu\text{m}$ . **B**, detail on isolated setae with fluffy apex (arrow) located at the periphery of an adhesive pad, in continuation with Oberhäutchen spinulae. Bar, 5  $\mu\text{m}$ . **C**, view of tail scale with indicated five sensory organs (arrowheads) localized along the front of the scale tip. Bar, 20  $\mu\text{m}$ . **D**, detail on a sensory organ with the central filaments (arrow). Bar, 5  $\mu\text{m}$ . **E**, detail showing a sensory organ with its sensorial filaments (arrow), located at the tip of a pad. Bar, 10  $\mu\text{m}$ . **Legends:** ob, Oberhäutchen; s, setae; sp, spinulae of the Oberhäutchen.

adhesion on the very irregular surfaces encountered in the arboreal environment by these geckos remains unknown, but it would deserve a specific analysis.

The proximal area of the pads, near the hinge region, is largely overlapped with the other pads, so cannot actively participate to the adhesion and is therefore devoid of setae. Only the distal region of the pad, the exposed area of the pads, actively interacts with the substrate, and therefore most setae of the mature outer generation are concentrated by the tip of the pad, like in the digits. During tail regeneration, the axial skeleton regenerated in this arboreal gecko is composed by an elastic cartilage, so that the new tails remains almost as flexible as the original one (Alibardi and Meyer Rochow, 1989; Alibardi and Meyer Rochow, 2017). The differentiation of elastic chondrocytes, initially noted for the New Zealand gecko *Hoplodactylus maculatus*, probably also occurs in other species of geckos with prehensile tails (Bauer, 1998), and appears as a generalized mechanism aiming to maintain tail efficiency despite the anatomical simplification of the regenerated tail that lacks of a segmented vertebral column. The extensive apical branching of caudal setae is comparable to that of digital pads, suggesting that caudal setae efficiently complement the adhesive behavior of these arboreal lizards (Bauer, 1998). The setae are likely shed from the apical region of the pad when the inner setae generation

is formed underneath, as previously indicated for digital scales in other geckos (Alibardi et al., 2007). The frequency of skin shedding in these pads however remains unknown.

The presence of numerous sensory organs, also in the regenerated scales and pads of the new tail, indicates that these mechanoreceptors are very important for recovering the orientation and maneuverability of the new tail in the arboreal environment. Similar sensory structures, indicated as tactile organs, have been described in other geckos where they regenerate after skin shedding (Hiller, 1977; von Düring and Miller, 1979). In conclusion, the present study further indicates that the cellular process of setae formation in geckos can be conveniently studied in the regenerating caudal pads (Alibardi and Meyer Rochow, 2017).

#### Acknowledgments

The study was mainly self supported (LA), including the immunohistochemical and TEM work. A. Bonfitto was supported by “Canziani Bequest” fund, University of Bologna [grant number A.31.CANZELSEW], Bologna, Italy.

## References

- Alibardi, L., 1999. Keratohyalin-like granules in embryonic and regenerating epidermis of lizards and *Sphenodon punctatus* (Reptilia, Lepidosauria). *Amphibia-Reptilia* 20, 11–23.
- Alibardi, L., Meyer-Rochow, V.B., 1989. Comparative fine structure of the axial skeleton inside the regenerated tail of lizards and the tuatara (*Sphenodon punctatus*). *Gegemb. Morphol. Jahrb (Leipzig)* 135, 705–716.
- Alibardi, L., 2003. Ultrastructural autoradiographic and immunocytochemical analysis of setae formation and keratinization in the digital pads of the gecko *Hemidactylus turcicus* (Gekkonidae, Reptilia). *Tiss. Cell* 35, 288–296.
- Alibardi, L., 2009. Cell Biology of adhesive setae in gecko lizards. *Zoology* 112, 403–424.
- Alibardi, L., 2010. Morphological and cellular aspects of tail and limb regeneration in lizard: a model system with implications for tissue regeneration in mammals. *Anat Embryol & Cell Biol* 207, 1–112.
- Alibardi, L., 2014. Presence of a glycine-cysteine-rich beta-protein in the oberhautchen layer of snake epidermis marks the formation of the shedding layer. *Protoplasma* 251, 1511–1520.
- Alibardi, L., 2018. Review: Mapping proteins localized in adhesive setae of the Tokay gecko and their possible influence on the mechanism of adhesion. *Protoplasma*. <https://doi.org/10.1007/s00709-015-0909-z>.
- Alibardi, L., Toni, M., 2006. Cytochemical, biochemical and molecular aspects of the process of keratinization in the epidermis of reptilian scales. *Prog. Histochem Cytochem* 40, 73–134.
- Alibardi, L., Meyer-Rochow, V.B., 2017. Regeneration of tail adhesive pad scales in the New Zealand gecko *Hoplodactylus maculatus* (Reptilia; Squamata; Lacertilia) can serve as an experimental model to analyze setal formation in lizards generally. *Zool. Res.* 38, 1–11.
- Alibardi, L., Spisni, E., Frassanito, A.G., Toni, M., 2004. Characterization of beta-keratins and associated proteins in adult and regenerating epidermis of lizards. *Tiss. Cell* 36, 333–349.
- Alibardi, L., Toni, M., Dalla Valle, L., 2007. Expression of beta-keratin mRNAs and proline-uptake in epidermal cells of growing scales and pad lamellae of gecko lizards. *J Anat* 211, 104–116.
- Arnold, E.N., 2002. History and function of scale microornamentation in lacertid lizards. *J. Morphol.* 252, 145–169.
- Autumn, K., Peattie, A.M., 2002. Mechanisms of adhesion in geckos. *Integr. Comp. Biol.* 42, 1081–1090.
- Autumn, K., Gravish, N., 2008. Gecko adhesion: evolutionary nanotechnology. *Phil. Trans. R. Soc. A* 366, 1575–1590.
- Bauer, A.M., 1998. Morphology of the adhesive tail tips of Carphodactylinae geckos (Reptilia: Diplodactylidae). *J. Morphol.* 235, 41–58.
- Bryant, S.V., Bellairs, A. d'A., 1967. Tail regeneration in the lizards *Anguis fragilis* and *Lacerta dugesii*. *Zool. J. Linnean Soc. (London)* 46, 297–305.
- Bellairs, A. d' A., Bryant, S.V., 1985. Autotomy and regeneration in reptiles. In: Gans, C., Billet, G.C.F. (Eds.), *Biology of the Reptilia*, vol. 15B. John Wiley & Sons, NY, USA, pp. 302–410.
- Carbone, G., Pierro, E., Gorb, S.N., 2011. Origin of the superior adhesive performance of mushroom shaped microstructured surfaces. *Soft Matter* 7, 5545.
- von Düring, M., Miller, M.R., 1979. Sensory nerve endings of the skin and deeper structures. In: Gans, C., Northcutt, R.G., Ulinski, P. (Eds.), *Biology of the Reptilia*, vol. 9 Neurology A. Academic Press, New York-San Francisco, USA, pp. 407–441.
- FitzSimons, V.F., 1943. *The Lizards of South Africa*. Transvaal Mus. Mem., Pretoria, pp. 1.
- Gao, H., Wang, X., Yao, H., Gorb, S., Artz, E., 2005. Mechanics of hierarchical adhesion structures of geckos. *Mech. Materials* 37, 275–285.
- Ge, L., Sethi, S., Ci, L., Ajayan, P.M., Dhinojwale, A., 2007. Carbon nanotube-based synthetic gecko tape. *PNAS* 104, 10792–10795.
- Hiller, U., 1972. Licht- und elektronenmikroskopische Untersuchungen zur Haftborstenentwicklung bei *Tarentola mauritanica* L. (Reptilia, Gekkonidae). *Z. Morph. Tiere* 73, 263–278.
- Hiller, U., 1977. Regeneration and degeneration of setae-bearing sensilla in the scales of the gekkonid lizard *Tarentola mauritanica* L. *Zool. Anz.* 199, 113–120.
- Irish, F., Williams, E., Seiling, E., 1988. Scanning electron microscopy of changes in epidermal structure occurring during the shedding cycle in squamate reptiles. *J. Morphol.* 197, 105–126.
- Liu, H.C., Maneely, R.B., 1969. Observations on the developing and regenerating tail epidermis of *Hemidactylus bowringi* (Gray). *Acta Anatomica* 72, 549–583.
- Maderson, P.F.A., 1964. Keratinized epidermal derivatives as an aid to climbing in gekkonid lizards. *Nature* 203, 780–781.
- Maderson, P.F.A., 1970. Lizard glands and lizard hands: Models for evolutionary study. *Forma Functio* 3, 179–204.
- Maderson, P.F.A., 1971. The regeneration of caudal epidermal specializations in *Lygodactylus picturatus keniensis* (Gekkonidae, Lacertilia). *J. Morph.* 134, 467–478.
- Maderson, P.F.A., Baranowitz, S., Roth, S.L., 1978. A histological study of the long term response to trauma of squamate integument. *J. Morphol.* 157, 121–136.
- Maderson, P.F., Rabinowitz, T., Tandler, B., Alibardi, L., 1998. Ultrastructural contributions to an understanding of the cellular mechanisms involved in lizard skin shedding with comments on the function and evolution of a unique lepidosaurian phenomenon. *J. Morphol.* 236, 1–24.
- Mertens, R., 1964. Der Eidechschenschwanz als Haftorgan. *Senckenbergiana biol.* 45, 117–122.
- Muller, L., 1910. Beiträge zur Herpetologie Kameruns. *Abh. Bayer. Akad. Wiss. (2. Kl.)* 24, 545–626.
- Niewiarowski, P.H., Stark, A.Y., Dhinojwale, A., 2016. Sticking to the story: outstanding challenges in gecko-inspired adhesives. *J. Exper. Biol.* 219, 912–919.
- Price, R.M., 1982. Dorsal scale microdermatoglyphics: ecological indicator or taxonomic tool. *J. Herpet.* 16, 294–306.
- Rizzo, N.W., Gardner, K.H., Walls, D.J., Keiper-Hrynko, N.M., Ganzke, T.S., Hallahan, D.L., 2006. Characterization of the structure and composition of gecko adhesive setae. *J. R. Soc. Interface* 3, 441–451.
- Russel, A.P., 2002. Integrative functional morphology of the gekkotan adhesive system (Reptilia: Gekkota). *Integr. Comp. Biol.* 42, 1154–1163.
- Scala, C., Cenacchi, G., Ferrari, C., Pasquinelli, G., Preda, P., Manara, G., 1992. A new acrylic resin formulation: a useful tool for histological, ultrastructural, and immunocytochemical investigations. *J. Histochem. Cytochem.* 40, 1799–1804.
- Schmidt, K.P., 1919. Contribution to the herpetology of the Belgian Congo based on the collection of the American museum Congo expeditions 1909-1915. Part 1. *Bull. Amer. Mus. Nat. Hist.* 39, 385–624.
- Tornier, G., 1899. Ein Eidechschenschwanz mit Saugscheibe. *Biol. Centralblatt* 19, 549–552.
- Wu, P., Alibardi, L., Chuong, C.M., 2014. Lizard scale regeneration and development: a model system to analyze mechanisms of skin appendages morphogenesis in amniotes. *Regeneration* 1, 16–26.